SIMULTANEOUS TEMPERATURE AND VELOCITY MEASUREMENTS IN A LARGE-SCALE, SUPERSONIC, HEATED JET

P.M. Danehy*, G. Magnotti+, D. Bivolaru+, S. Tedder*, A.D. Cutler+
*NASA Langley Research Center
Hampton, Virginia
+The George Washington University
Newport News, Virginia

ABSTRACT

Two laser-based measurement techniques have been used to characterize an axisymmetric, combustion-heated supersonic jet issuing into static room air. The dual-pump coherent anti-Stokes Raman spectroscopy (CARS) measurement technique measured temperature and concentration while the interferometric Rayleigh scattering (IRS) method simultaneously measured two components of velocity. This paper reports a preliminary analysis of CARS-IRS temperature and velocity measurements from selected measurement locations. The temperature measurements show that the temperature along the jet axis remains constant while dropping off radially. The velocity measurements show that the nozzle exit velocity fluctuations are about 3% of the maximum velocity in the flow.

INTRODUCTION

Designers of hypersonic air-breathing engines extensively use computational fluid dynamic (CFD) codes based on the Reynolds Average Navier Stokes (RANS) equations. These codes typically model turbulence with algebraic (zero equation) or two-equation models that were originally developed for subsonic, non-reacting flow and modified for use in supersonic reacting flow. This approach results in numerous difficulties and inaccuracies when applied to predict supersonic combustion, for example in predicting turbulence-chemistry interactions and turbulent scalar transport.[1] Higher-order turbulence models can potentially improve on this approach. In particular, new models are required to better reproduce the turbulent mass and energy transfer, as well as the turbulence-chemistry interactions.[1] However, these models need to be calibrated and validated empirically using quantitative flowfield data such as temperature, concentration and velocity measurements.

Quantitative flowfield measurements in supersonic combustors are very difficult to perform because of the severe testing environment and limited optical access. The flow is typically contained within a duct, requiring windows for optical measurements. These windows are subjected to high thermal and mechanical stresses, sometimes resulting in failure. They can also become dirty or can be covered with water vapor droplets, preventing transmission of laser beams. The coherent anti-Stokes Raman spectroscopy (CARS) method is one of the most widely used optical measurement technologies for studying ducted supersonic combustion flows.[2,3,4,5,6,7,8,9,10] CARS, which measures temperature and sometimes gas concentrations, often uses two small round or slotted windows located on opposite sides of the duct. At NASA Langley Research Center, a series of experiments[2,7,9,10] have been performed in a supersonic combustor using broadband CARS and the dual-pump CARS technique originally developed by Lucht.[11] Dual-pump CARS allows single-point simultaneous measurements of temperature and concentration of N_2, O_2 and H_2. A limitation of CARS is that the flow velocity cannot be easily measured. Recently, we have developed an Interferometric Rayleigh scattering (IRS) velocity measurement system that observes the scattering from the green CARS pump beam.[12] IRS velocimetry was previously pioneered at the NASA Glenn Research Center by Seasholtz and

coworkers[13,14] and also advanced by others.[15,16] We have adapted the IRS measurement technique to study combustion flows.[17] Combining the CARS and IRS techniques allows us to simultaneously measure temperature, velocity and concentration, and thereby evaluate the statistical quantities (means, variance, covariance, etc.) that can validate and improve turbulence models.[17]

A limitation of the IRS method is that it requires much greater optical access than CARS. For the present experiment, specific hardware was developed to generate a flowfield amenable to the both CARS and IRS measurement techniques while being relevant to the CFD community. An unducted axisymmetric coaxial jet was chosen because of the excellent optical access and symmetry, which reduces the quantity of data required to fully characterize the flowfield. A small-scale (10 mm diameter nozzle exit) axisymmetric supersonic burner was initially developed and tested to reduce risk, validate the design of the hardware, establish test conditions and to provide a test case to demonstrate the newly developed CARS-IRS technique.[18,19] Based on the success and lessons learned from these experiments, a 6.35 times larger axisymmetric jet was fabricated and installed in a large-scale supersonic combustion test facility and was tested.[20] This paper reports a preliminary analysis of the CARS-IRS measurements obtained in this large scale facility.

EXPERIMENTAL SETUP

FACILITY, TEST HARDWARE, AND OPERATING CONDITIONS

The experiments were performed in the NASA Langley Research Center Direct Connect Supersonic Combustion Test Facility. This facility mixes air, oxygen, and hydrogen in a combustion chamber to produce a mixture of heated gas (vitiated air), containing the same O_2 mass fraction as air but with excess water vapor. The heated gas exhausts into the room through a Mach 1.6 nozzle.[20] The nozzle exit diameter is 6.35 cm. The test hardware is designed to have an optional annular coflow (co-axial flow) of fuel or inert gas. Test were conducted at enthalpy Mach number M_h=5.5, meaning that the sensible enthalpy of the test gas is the same as air in the reference frame of a vehicle flying at that Mach number. Two cases were investigated in detail with the CARS-IRS system; the first, a case of mixing (between jet and ambient air) in which there is no coflow, and the second a case in which the coflow is H_2 with an overall equivalence ratio ϕ = 1. (In other words, the rate of coflow of H_2 is exactly the amount required to combine with all the unreacted O_2 in the center jet to form H_2O.) The average and the standard deviation of the variation of facility flow rates and total pressure (including variation within runs and from run to run) are: air flow = 0.920±0.012 kg/s, O_2 flow = 0.155±0.005 kg/s, H_2 flow = 0.0147±0.0004 kg/s, 414±27 kPa. For runs with H_2 coflow: coflow = 0.032±0.004 kg/s. (Uncertainties are given for the 95% probability limits throughout this paper.) While CARS-IRS data were obtained for both cases shown in Figure 1, only CARS-IRS measurements from case B.a are shown in this paper.

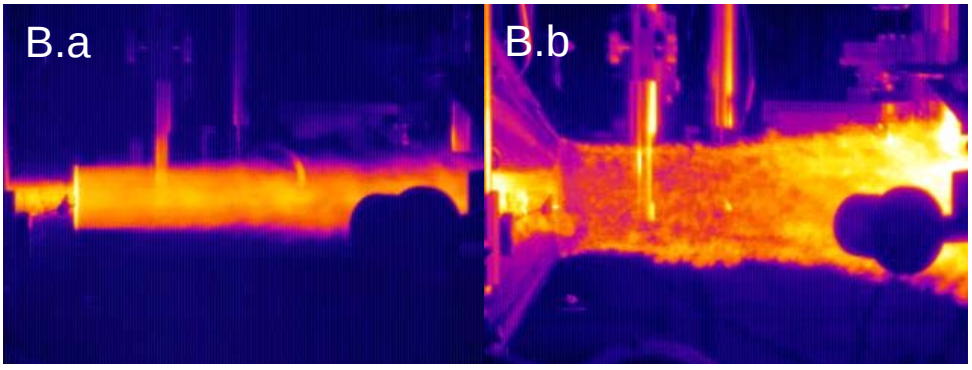

Figure 1. IR images of large scale flame during facility operation, cases B.a (M_h=5.5), and B.b (M_h=5.5, H_2 coflow at ϕ=1) from Reference 20. The flow is from left to right. Silhouettes and reflections of optical hardware can be seen in the images.

EXPERIMENT DESIGN

The order of sampling and the number of measurements made at each point were chosen using classical methods of experiment design, such as randomization, blocking, and replication.[21] Randomization was applied to minimize the effects of consistent errors from run-to-run, from day-to-day, and as a function of elapsed time from facility startup, due, for example, to variable facility flow rates, heating of the model, differences in instrumentation setup, etc. Blocking was applied to identify underlying day-to-day trends. Replication was applied to allow checking of models for the response variables, i.e., the statistical parameters of the CARS-IRS system measurements of interest, such as means, variances, covariances, etc. The location of measurement points was selected to enable several types of analytical functions to be used in creating surface fits to the response variables. Points were concentrated in regions of high gradient in the response variables. Numbers of samples at a point were selected so statistical parameters could be computed with random error (i.e., error due to insufficient numbers of samples for the statistics to be fully converged) no worse than the estimated precision inherent in the instrument. More details on the experimental matrix will be provided in future publications.

CARS AND RAYLEIGH SETUP AND ANALYSIS METHODS

The combined CARS-IRS apparatus has been described in detail in Reference 22. A brief summary will be provided here. The CARS system uses three laser beams of different colors: 532 nm generated by an injection-seeded Nd:YAG laser, 553 nm generated by a narrow-band dye laser pumped by the Nd:YAG, and 603 nm from a broadband dye laser, also pumped by the Nd:YAG. Using the dual-pump CARS method, these three colors simultaneously probe N_2, H_2 and O_2 Raman resonances.[9,18] These three lasers are mounted on a mobile double-decker cart located in the basement below the test facility. The three beams are transmitted into the test cell through a hole in the floor using 3-inch diameter mirrors. Inside the test cell, they are transmitted by a series of mirrors to the side of the jet. The beams are combined together using three pairs of mirrors as shown in Figure 2, and then pass through a lens, which focuses the beams at a point in the flow known as the measurement volume. Interaction between the three beams and the gas within the measurement volume generates a fourth beam, which is detected by a spectrometer equipped with a CCD camera. By analyzing the measured CARS spectrum, the gas temperature and N_2, H_2 and O_2 mole fractions can be determined in the measurement volume. The relay mirrors, transmission optics and collection optics are attached to a large structure that can be translated in three dimensions using servo motors. The measurement volume can probe different locations in the flow during a facility run. In the present experiment, all measurements were obtained in a horizontal plane passing through the axis of the jet.

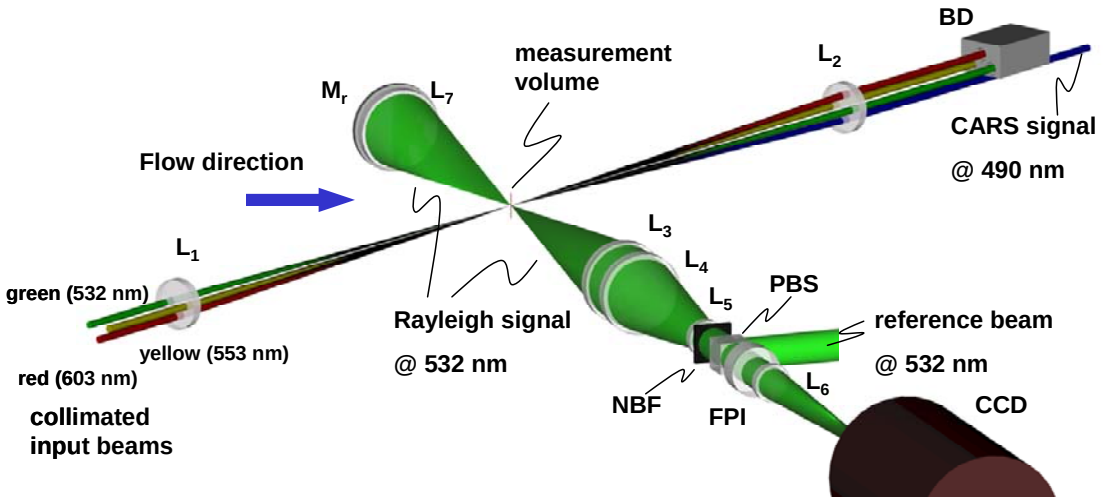

Figure 2. Experimental Setup for CARS and IRS measurement systems.

Figure 3 shows two examples of CARS spectra obtained in the combustion heated supersonic jet. The data points show peaks from N_2 (right side of each spectrum) and O_2 (left). No H_2 spectral lines were observed in this experiment because all the H_2 in the center jet was consumed in the heater section of the facility and no additional H_2 was added in the coflow. A spectrally-broad CARS signal is also observed in the spectra, originating from non-resonant contributions from all the molecules present in the measurement volume. The data have been fit with a theoretical spectral analysis code, known as CARSFIT, from Sandia National Laboratories and modified by us.[9] In our first series of dual-pump CARS measurements and analyses,[9,10] CARSFIT was used to generate a quick-fitting spectral library. An interpolation code successfully allowed measurements to be obtained between library entries. During the recent[18] and present data analysis, this method resulted in an unphysical clustering of temperature measurements not observed in our prior measurements[9,10] obtained with a different CARS system. Consequently, we used an alternate approach: CARSFIT's internal iterative fitting algorithm was used to minimize the difference between the data and the fit.[23,24] A Linux batch file was used to execute CARSFIT's iterative method for each measurement point. Since no H_2 was present in the fits, the main fit parameters were temperature, N_2 and O_2 concentration. Spectra were peak-normalized before fitting. Fits resulting in a chi-squared error of greater than one were rejected to remove erroneous fits, usually resulting from low signal intensity. Using this method on a single processor computer, a typical run containing 1000 spectra could be fit in less than a day. However, not all the spectra could be fit due to time constraints, so only a small fraction of the data set is presented in this paper. Furthermore, at the present time, different analysis techniques are being evaluated which affect the composition measurements, though they have less impact on fitted temperatures. Consequently, only CARS temperatures are reported herein. These temperature measurements should be considered preliminary. As the analysis methods mature, the data will be reanalyzed and presented in future reports.

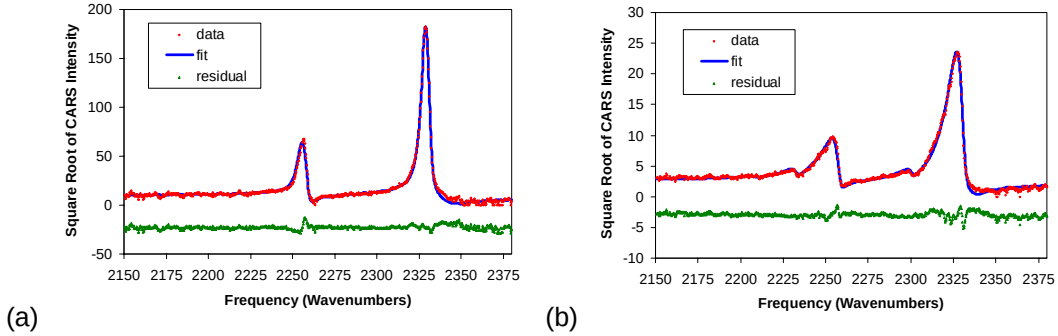

Figure 3. Measured CARS spectra, best fits, and residuals (offset by a constant) for two single-shots during Run 69, resulting in fitted temperatures of (a) 303 K and (b) 1154 K.

The interferometric Rayleigh scattering (IRS) measurement system is also shown in Figure 2. Lens L_3 collects 532 nm Rayleigh scattered light from the measurement volume and a pair of lenses down-collimates this light. It then passes through a narrowband filter (NBF), a Fabry-Perot interferometer (FPI) and another lens onto a CCD camera. The FPI etalon spectrally disperses the Rayleigh scattered light on the CCD, shown as horizontal patterns in Figure 4(a). A frequency reference signal is directed simultaneously into the optical path, resulting in concentric fringes (ring patters) shown in the figure. The two horizontal bands are the Rayleigh scattered light from laser beams originating from two different collection angles which are parallel but opposite. The radial velocity component is determined from backward Rayleigh scattering, collected at an angle of 120±1 degrees between incident and collected wave vectors. The axial velocity component is determined from forward Rayleigh scattering collected by lens L_7 shown in Figure 2 mounted directly across from the backward scattering collection optics. This backward scattering is collected with an angle of 60 degrees between incident and collected wave vectors. A normal incidence mirror, M_r, is placed just after the lens to reflect the forward scattering back through the collection lens then direct it down the same optical path as the backward scattering as detailed in Reference 25. These two patterns are optically adjusted to appear spatially

separated on the CCD camera, as shown in Figure 4. Since these two scattered light vectors are in opposite directions, they are sensitive to orthogonal velocity components through the Doppler shift effect.[12] The measurement system was oriented with respect to the flow so that one of measured components was along the flow axis and the other measured component was perpendicular to the axis. For each bright region along the horizontal line in Figure 4(a) a measurement of velocity can, in principle, be obtained. Thus by analyzing these spectra, two components of velocity can be measured at multiple spatial locations along the laser beam.

To process these spectra, a sequence of steps must be performed, as described in Reference 12. Very briefly, the center of the reference fringes is found, the images are converted from (x-y) coordinates into a (y-Θ) coordinate system and summed into a single row for each velocity component. Then the spectra are linearized and calibrated using the known properties of the etalon. Next, Gaussian functions are fit to the reference and the signal to determine the Doppler shift as shown in Figure 4(b). Finally, these Doppler shifts are converted to velocity in m/s using information from the experiment, such as the angle between the incident laser beam and the collected scattering. By design, the instrument requires that the ratio of reference to Rayleigh signal amplitudes approaches unity. This is because the spectra can be most easily fit (with minimum errors in finding the Doppler shift) if the amplitudes of signal and reference are similar. Unfortunately, for most of the tunnel runs of the present test, the reference signal was about an order of magnitude smaller than the Rayleigh signal. Also, in the presence of particulates, the reference signal was about an order of magnitude larger than the Rayleigh signal. Analysis methods that are robust enough to fit these data are presently under development. Consequently, in this paper, only velocity measurements nearest the nozzle exit are reported because those spectra had signal and reference amplitudes of similar magnitudes. Future papers will report the downstream data.

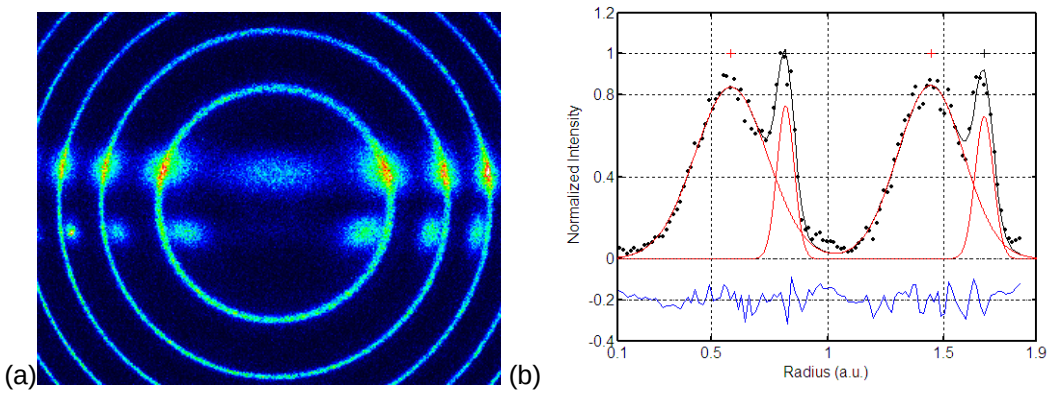

Figure 4 . Rayleigh scattering interferogram (a) and linearized spectrum and best fit (b). The spatial width of the image in (a) is about 2 mm. The plot in (b) shows the experimental data (black symbols), the theoretical best fit (black line), and the residual between them (blue), offset by a constant. The fit functions are Gaussian functions (red lines) with the narrow peak being at the laser frequency.

RESULTS

CARS TEMPERATURE MEASUREMENTS

Figure 5 and Table 1 summarize the temperature measurements obtained with CARS at selected points in the flowfield. These measurements should be considered preliminary. Improved analysis techniques are currently being developed to improve the accuracy and precision of the measurements. Nonetheless, review of the preliminary measurements provides useful insights into the flowfield and also helps to identify parts of the CARS (and IRS) data analysis that need improvement. Figure 5 shows CARS data from three tunnel runs obtained on

the same day. Each run was broken up into 4 measurement locations, though run 64 repeated the same measurement location twice. The measurement points analyzed were mainly at three axial distances downstream of the nozzle exit.

Looking first at the on-axis point closest to the nozzle exit, the temperature is 991 Kelvin with a standard deviation, σ = 110 Kelvin. The statistical uncertainty in this mean is ±20 Kelvin, as shown in Table 1. (The statistical uncertainty in the mean is computed from $2\sigma/n^{1/2}$, where n is the number of samples in the average. This statistical uncertainty does not include other errors in the experiment, such as systematic errors or run-to-run errors.) As the gas travels further downstream, the mean temperature remains constant, location-to-location, considering the statistical uncertainty. The slight rise in measured values with downstream distance is probably insignificant. The standard deviation along the flow axis also remains roughly constant. Measurements well outside the jet show mean temperatures between 255 and 279 Kelvin. Along radial profiles in the flow, the temperature drops monotonically from a maximum value at the center of the jet to a minimum value in the ambient gas, as expected for a heated, non-reacting jet. The standard deviation, however, increases in the shear layer between the jet and the ambient gas, reaching a maximum about 25% larger than on the centerline.

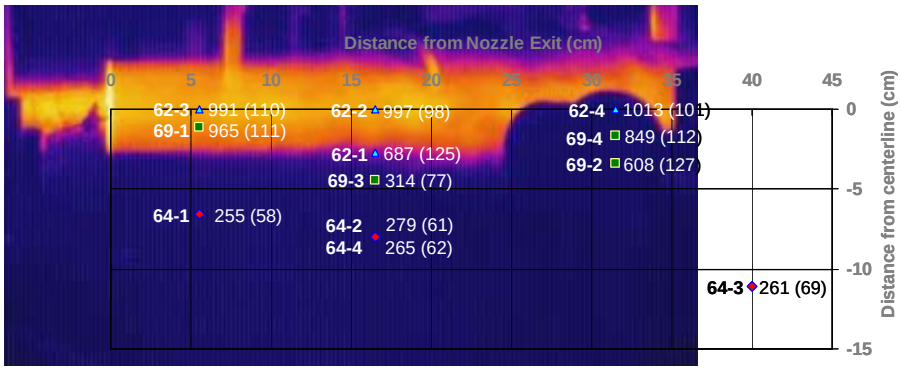

Figure 5. Graphical summary of CARS temperature measurements. Symbols represent measurement locations. The numbers to the left of the symbols represent the run and point number. The mean temperature is shown to the right of the symbol and the standard deviation is shown in parentheses.

Run 62, Block 35

Point Number	Mean T (Kelvin)	Std. Dev. T (Kelvin)	Std. Dev. T (%)	No. of Shots	Unc. in Mean (95%, Kelvin)	Axial Pos. (cm)	Radial Pos. (cm)
62-1	687	125	18	130	22	16.5	-2.7
62-2	997	98	10	134	17	16.5	0.0
62-3	991	110	11	115	20	5.5	0.0
62-4	1013	101	10	147	17	31.5	0.0

Run 64, Block 37

Point Number	Mean T (Kelvin)	Std. Dev. T (Kelvin)	Std. Dev. T (%)	No. of Shots	Unc. in Mean (95%, Kelvin)	Axial Pos. (cm)	Radial Pos. (cm)
64-1	255	58	23	136	10	5.5	-6.6
64-2	279	61	22	165	9	16.5	-8.0
64-3	261	69	27	137	12	40.0	-11.1
64-4	265	62	23	163	10	16.5	-8.0

Run 69, Block 42

Point Number	Mean T (Kelvin)	Std. Dev. T (Kelvin)	Std. Dev. T (%)	No. of Shots	Unc. in Mean (95%, Kelvin)	Axial Pos. (cm)	Radial Pos. (cm)
69-1	965	111	11	100	22	5.5	-1.1
69-2	608	127	21	151	21	31.5	-3.4
69-3	314	77	24	151	12	16.5	-4.4
69-4	849	112	13	155	18	31.5	-1.7

Room Air

Calibration	Mean T (Kelvin)	Std. Dev. T (Kelvin)	Std. Dev. T (%)	No. of Shots	Unc. in Mean (95%, Kelvin)	Axial Pos. (cm)	Radial Pos. (cm)
Room Air	284	26	9	952	2	n/a	n/a

Table 1. Summary of Preliminary CARS Temperature Measurements from selected runs.

Figure 6 shows probability density functions (PDFs) for a measurement in static room air and three selected points in the flow. The data have been distributed into 50 Kelvin bins with the numerical labels on the horizontal axes indicating the highest temperature in each bin. Figure 6(a) shows a very narrow distribution of measurements around room temperature. The mean and standard deviation for these room temperature air measurements were 284 Kelvin and 26 Kelvin, respectively. Figure 6(b) shows a measurement point well outside the jet which has a mean and standard deviation of 279 Kelvin and 61 Kelvin, respectively. Figure 6(c) shows the broadest PDF obtained in the experiment, which was measured in the jet's shear layer. Finally Figure 6(d) shows the temperature distribution at the point closest to the nozzle exit. The PDFs are generally Gaussian in nature, although Figure 6(d) is slightly skewed towards lower temperatures. Approximately 10 times as much data as this has been obtained at each one of these measurement locations but has not yet been analyzed, so more concrete conclusions can be drawn from the complete data set.

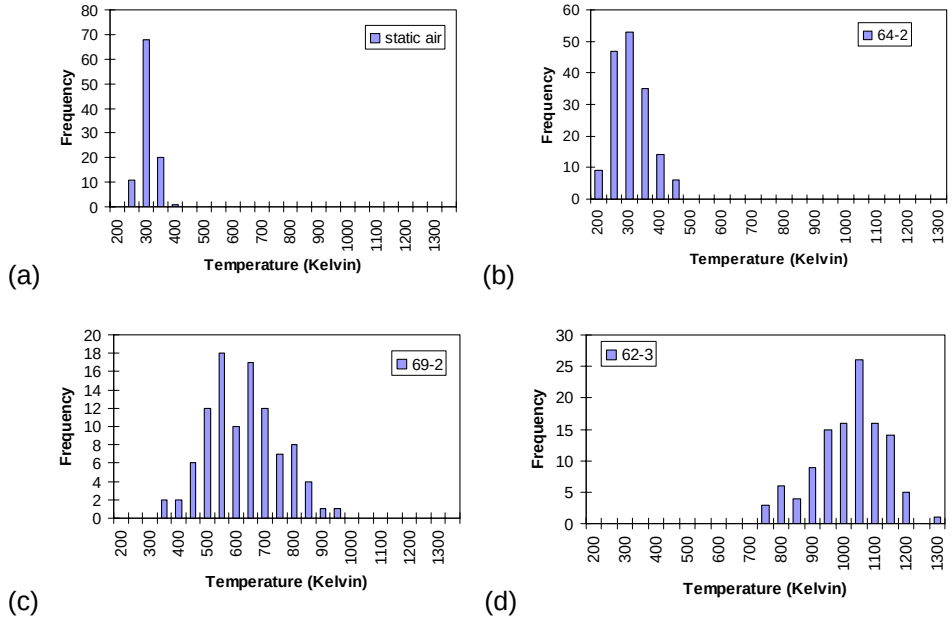

Figure 6. Histograms of CARS temperatures obtained in (a) static room air and points (b) far outside the jet (Run 64, Point 2), (c) in the shear layer (Run 69, Point 2) and (d) close to the nozzle exit (Run 62, Point 3).

The measurements obtained in the ambient air furthest from the jet axis appear to show a systematic error compared to the expected temperatures which should be near the ambient 297±2 Kelvin temperature measured on the day of the experiment. The air around the jet enters the test facility from the outside and is accelerated by the facility ventilation system and also by entrainment with the jet flow, lowering the temperature of this gas. However, to achieve a mean temperature of 255 K (Run 64, Point 1), the room temperature air would need to be expanded isentropically to nearly Mach 1, which is unlikely. If the air near the jet is accelerated by entrainment to a more modest 100 m/s (approximately Mach 0.3), for example, then the temperature would be expected to drop about 2% based on an isentropic expansion, resulting in an expected temperature of 291 Kelvin – still much higher than the measured mean temperatures. All the measured temperatures from outside the jet are well below room temperature, indicating a probable systematic error in the measurement. Comparisons with additional measurements and also with CFD analyses of the facility flow will provide additional information to determine if these data points show a systematic error. During the CARS data analysis, a measured spectrum obtained in room-temperature air is usually best fit to determine the instrument function of the spectrometer / camera system.[9] This procedure acts to calibrate the measurement system at low temperatures where the width of the CARS signal is the primary

indicator of temperature. At higher temperatures, the temperature sensitivity of CARS spectra is mainly derived from the ratio between the two vibrational bands of both nitrogen and oxygen (seen to the left of the main N_2 peak in Figure 3(b)). We are assessing the possibility that the curvature of the jet acts as a lens adjusting the focus of the CARS signal on the spectrometer, altering this instrument function during measurements. Fluctuations in the jet can cause the focus to change on the CCD camera, resulting in an apparent temperature change during the analysis of cold CARS spectra. This would explain the larger standard deviation measured in run 64 compared to measurements in static room air on the same day. In future analysis we will investigate using one of the points obtained outside the jet during a tunnel run such as Run 64 as our calibration point, thereby removing the systematic error in the mean temperature, though not reducing the standard deviation. Blurring on the CCD camera was observed in prior work.[9] To reduce this problem in the current work, a new grating was purchased and installed in the spectrometer to provide more than twice the dispersion, reducing the width of the instrument function. This change should have reduced the effect of blurring but in this fluctuating flow field, the problem was clearly not eliminated. In the future, even higher spectral resolution could be used to further reduce blurring and improve the absolute accuracy and precision of the temperature measurements. Alternately, a different CARS approach, such as pure rotational CARS, which is much more sensitive at lower temperatures, could be used.[26] However, pure rotational CARS is less sensitive to temperature at high temperatures than vibrational CARS.

Regarding the standard deviation in the measured temperatures, some of the fluctuations are caused by flow unsteadiness and some are caused by the CARS instrument. In a fuel-lean laminar hydrogen-air flame, the same CARS instrument measured a standard deviation of 65 K at 900 K, which is close to the nozzle exit temperature. This can be regarded as an estimate of the instrument precision at this temperature. If we assume that the instrument error and the unsteady fluctuations in the flow are uncorrelated, then they add in quadrature. Thus, the estimated temperature standard deviation in the flow is about 88 Kelvins, or 9% of the freestream temperature. This should be regarded as an upper estimate of the temperature fluctuations because, as shown in the comparison in Figure 6(a) and (b), CARS temperature measurements obtained during facility operation have additional random error compared to quiescent measurements. These errors will be further characterized and quantified, if possible, in future work.

The CARS signal exhibited an unusually large signal variation in this experiment compared to our prior work. This was caused primarily by laser beam steering by the strong density gradients between the heated jet and the relatively cool ambient gas, particularly in the turbulent shear layer. Either the three beams did not cross reliably and did not generate a CARS signal, or the CARS signal was generated but was deflected away from the spectrometer and camera. Roughly 5% of the CARS spectra saturated the CCD camera while a few percent of the time, no CARS signal was observed, demonstrating a range in intensity of > 1000. Thus far, about 75% of the CARS spectra from a given measurement location could be well fit to determine temperature in the current experiment. Such fluctuations and signal dropouts could potentially impact the accuracy of mean temperatures in this experiment because the CARS signal intensity drops rapidly with increasing temperature. Based on a theoretical calculation using constant composition and varying the temperature,[27] the peak nitrogen CARS signal shows a temperature dependence of $T^{-3.5}$, graphed as the solid line in Figure 7. If the CARS signal intensity is low, then high-temperature spectra can fall below the detection limit and get excluded from calculation of the mean. If high-temperature spectra are excluded, then the mean will have a bias towards lower temperature.

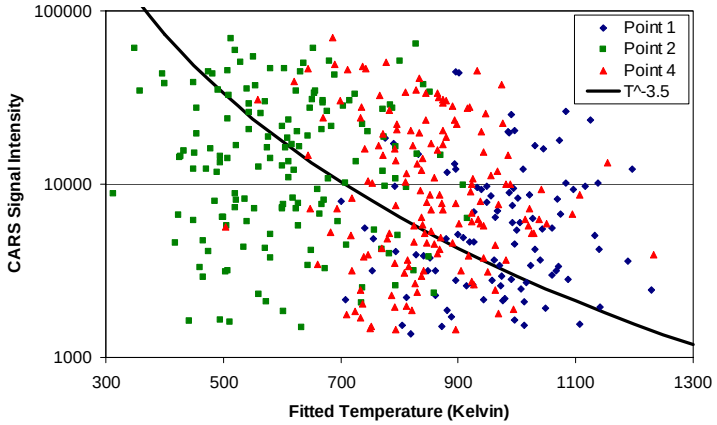

Figure 7. Comparison between measured CARS signal and fitted CARS temperatures for three measurement locations in Run 69. The arbitrarily scaled black curve shows the expected temperature dependence of the peak CARS signal due only to temperature effects.

Figure 7 shows data plotted to investigate whether a systematic error in mean temperature was obtained in this experiment. The CARS signal intensity is graphed versus the fitted temperature for each of several hundred single-shot temperature measurements in the flow. If the data points follow the trend shown by the black curve, then lower signal intensity shots would correspond to higher temperatures. If this were the case, and if the lower signal intensity shots were excluded, there would be a bias error. However, the data appear to be nearly uncorrelated with the curve in Figure 7. Low temperature spectra are just as likely to have low signal as high temperature spectra. Consequently, we believe that the bias error due to excluding 25% of the data in the present analysis is negligible. For further quantitative proof of validity of this claim we calculated the mean temperatures for three points in Run 69 by using all the successfully fitted temperature data and comparing that to the mean calculated after excluding the shots having the next lowest 25% of signal intensity. The result of this calculation is shown in Table 2. Removing data changed the temperature a negligible amount, quantitatively indicating that the bias error is negligible.

	mean of all T data with chisqr < 1 (Kelvin)	mean of T data after 25% lowest signal shots removed (Kelvin)
Point 1	965	970
Point 2	608	605
Point 4	849	852

Table 2. Results of bias error study. "T" is temperature.

We estimate the systematic errors in the CARS temperature measurements to be as large as 80 K based on comparisons between measured CARS temperatures in a laminar flat flame burner and a chemical equilibrium calculation that predicts the temperature in this flame. We expect to be able to reduce this error through improved CARS analysis methods.

IRS VELOCITY MEASUREMENTS

Table 3 shows the preliminary IRS velocity measurements obtained simultaneously with the CARS measurements and analyzed thus far. Measurements from one point each for two runs are shown. Both measurement points are nearest the nozzle exit where signal-to-reference amplitude was optimal. In each interferogram, measurements were obtained at four locations (all within 2 mm) along the laser beam near its focus, but only measurements from a single IRS measurement point are presented here. The axial velocity for Run 62, Point 3, which is nearest

the nozzle exit and on the flow axis, is 1132 m/s with a standard deviation of 47 m/s. The radial velocity at the same point was 77 m/s with a standard deviation of 42 m/s, indicating that the measurement location was either off the center line or that it has a systematic error. A calibration data run, obtained using a low flowrate of air with an expected radial velocity close to zero showed a 4 m/s mean velocity. This evidence suggests that the 'zero' for the instrument is accurate to within roughly 10 m/s. If the sensitivity vector of the Rayleigh scatting was not oriented exactly perpendicular to the flow axis, this could cause a systematic error in measured radial velocities. Such errors will be studied and quantified in future work.

An estimate of the instrument precision can be obtained from the determination of the free spectral range of the etalon during image processing of the Rayleigh spectra.[12] The variation around its mean is converted from frequency into velocity (in m/s) specific to each component. In this way, the instrument precision is estimated to be 18 m/s for the radial component and 31 m/s for the axial component of velocity. If we again assume that the actual velocity fluctuations in the flow are uncorrelated with instrument error, then these terms add in quadrature to show the overall standard deviation. Thus the best estimate for the true axial velocity fluctuations is 35 meters per second, or 3% of the measured velocity. For the radial component, the estimated velocity fluctuations are 38 m/s.

Point Number	Velocity Component	Mean Vel (m/s)	Std. Dev. (m/s)	Std. Dev. (%)	No. of Shots	Unc. in Mean (95%, m/s)	Axial Pos. (cm)	Radial Pos. (cm)
62-3	axial	1132	47	4	139	8	5.5	0.0
69-1	axial	1185	45	4	188	7	5.5	-1.1
62-3	radial	77	42	n.a.	170	6	5.5	0.0
69-1	radial	88	30	n.a.	172	5	5.5	-1.1

Table 3. Summary of preliminary IRS velocity measurements at two locations.

Figure 8 shows histograms for the two measurements summarized in Table 3. The distribution of measurements looks Gaussian in each case. Prior comparisons between these measurements and an axisymmetric CFD simulation of the flow field showed agreement in the axial velocity, though the radial velocity was larger than the CFD predited.[12] Presently the velocity measurements could have systematic errors as large as 80 m/s, though improvements to the software analysis may allow these systematic errors to be corrected and reduced in the final analysis of the data.

Measurements obtained further downstream had excellent signal-to-noise ratio but because of the low intensity of the reference signal have proved difficult to analyze thus far although progress is being made towards fitting them.

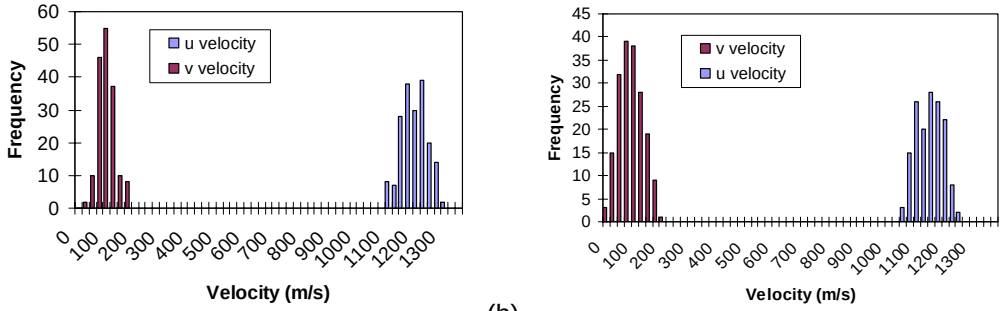

(a) (b)

Figure 8. Histograms of Rayleigh Velocity Measurements for (a) Run 69, Point 1 and (b) Run 62, Point 3.

SUMMARY AND CONCLUSIONS

This paper reports a preliminary analysis of velocity and temperature measurements obtained in a combustion-heated axisymmetric free jet. Only a limited fraction of the data set has been analyzed thus far, so caution should be exercised when drawing conclusions. In summary, the mean CARS temperature showed negligible variation with distance between 1 and 6 nozzle diameters downstream of the nozzle exit. Radial profiles of temperature showed an expected monotonic change in temperature from high temperature in the center of the jet to low temperature in the ambient. Temperature standard deviations remained roughly constant with downstream distance while they increased in the shear layer and reached a minimum outside the jet. Methods for evaluating and reducing systematic errors and improving the CARS data analysis were discussed. The velocity measurements near the nozzle exit showed a smaller standard deviation than the temperature measurements. The estimated velocity fluctuations, based on the standard deviation were about 3% of the mean axial velocity. Preliminary comparisons can be made between this data set and computational fluid dynamics codes in an effort to verify assumptions used in the codes. But final conclusions should not be drawn until the comparisons are made with the complete data set.

ACKNOWLEDGMENTS

We wish to acknowledge the important contributions to the work from Diego Capriotti, Tom Mills and Barry Lawhorne and his team who operate NASA Langley's Direct Connect Supersonic Combustion Test Facility. We also appreciate the contributions from Stephen Jones, Joseph Lee, Lloyd Wilson, Markus Weikl and James Downey, who assisted in building the CARS-IRS apparatus and installing it in the facility. This work was supported by NASA's Fundamental Aeronautics Program's Hypersonics Project, Experimental Capabilities Discipline and also by the Defense Test Resource Management Center's (DTRMC) Test and Evaluation/Science and Technology (T&E/S&T) program, under the Hypersonic Test focus area.

REFERENCES

[1] Baurle, R.A., "Modeling of High Speed Reacting Flows: Established Practices and Future Challenges," AIAA 2004-267, 42nd Aerospace Sciences Meeting and Exhibit, Reno, NV, 5-8 Jan, 2004.

[2] Anderson, T.J. and Eckbreth, A.C., "Simultaneous coherent anti-Stokes Raman spectroscopy measurements in hydrogen-fueled supersonic combustion", *Journal of Propulsion and Power,* Vol. 8, No. 1, 1992, pp. 7-15.

[3] Smith, M.W., Jarratt, O. Jr., Antcliffe R.R., Northam, G.B., Cutler, A.D. and Taylor, D.J., "Coherent anti-Stokes Raman spectroscopy temperature measurements in a hydrogen-fueled supersonic combustor," *Journal of Propulsion and Power*, Vol. 9, No. 2, 1993, pp. 163 –168.

[4] Weisgerber, H., Fischer, M., Magens, E., Winandy, A., Foerster, W., Beversdorff, M., "Experimental analysis of the flow of exhaust gas in a hypersonic nozzle," AIAA Paper 98-1600, 8th International Space Planes and Hypersonic Systems and Technologies Conference, Norfolk, Virginia, USA, 27-30 April, 1998.

[5] Yang, S.R., Zhau, J.R., Sung, G.J. and Yu, G., "Multiplex CARS measurements in supersonic hydrogen/air combustion," *Applied Physics B*, Vol. 68, 1999, pp. 257-265.

[6] Vereschagin, K.A., Smirnov, V.V., Stelmakh, O.M., Fabelinski, V.I., Sabelnikov, V.A., Ivanov, V.V., Clauss, W. and Oschwald, M., "Temperature measurements by coherent anti-Stokes Raman spectroscopy in hydrogen-fuelled scramjet combustor," *Aerospace Science and Technology*, Vol. 5, 2001, pp. 347-355.

[7] Grisch, F., Bouchardy, P. and Clauss, W., "CARS Thermometry in high pressure rocket combustors," *Aerospace Science and Technology*, Vol. 7, 2003, pp. 317-330.

[8] Cutler, A.D., Danehy, P.M., Springer, R.R., O'Byrne, S., Capriotti, D.P., DeLoach, R., "Coherent Anti-Stokes Raman Spectroscopic Thermometry in a Supersonic Combustor," AIAA J., Vol. 41, No. 12, Dec. 2003.

[9] S. O'Byrne, P. M. Danehy, S. A. Tedder, and A. D. Cutler, "Dual-Pump Coherent Anti-Stokes Raman Scattering Measurements in a Supersonic Combustor" AIAA Journal Vol. 45, No. 4, p. 922-933, April 2007.

[10] S. A. Tedder, S. O'Byrne, P. M. Danehy, A. D. Cutler "CARS Temperature and Species Concentration Measurements in a Supersonic Combustor with Normal Injection", AIAA Paper 2005-0616, 43rd Aerosciences Meeting and Exhibit, Reno NV, Jan 10-13, 2005.

[11] R.D. Hancock, F.R. Schauer, R.P. Lucht, R.L. Farrow, "Dual-pump CARS measurements of nitrogen and oxygen in a laminar jet diffusion flame," Appl. Opt. 36, pp. 3217-3226, 1997.

[12] D. Bivolaru, P. M. Danehy, R. L. Gaffney, Jr. and A. D. Cutler, "Direct-View Multi-Point Two-Component Interferometric Rayleigh Scattering Velocimeter," 46th AIAA Aerospace Sciences Meeting and Exhibit 7 - 10 January 2008, Reno, Nevada, AIAA Paper 2008-236

[13] Seasholtz, R. G., Zupanc, F. J. and Schneider, S. J., "Spectrally Resolved Rayleigh Scattering Diagnostics for Hydrogen-Oxygen Rocket Plume Studies," *J. Propulsion and Power,* Vol. 8, No. 5, 1992, pp. 935-942.

[14] Seasholtz, R. G., Buggele, A. E. and Reeder, M., *"Instantaneous Measurements in a Supersonic Wind tunnel Using Spectrally Resolved Rayleigh Scattering,"* Proceedings of the International Symposium on Optical Science, Engineering and Instrumentation, Society of Photo-Optical Instrumentation Engineers, Bellingham, WA, 1995

[15] A. Mielke, K. Elam, and C. Sung, "Molecular Rayleigh Scattering Diagnostic for Dynamic Temperature, Velocity, and Density Measurements," AIAA-2006-2969, *25th AIAA Aerodynamic Measurement Technology and Ground Testing Conference*, San Francisco, California, June 5-8, 2006.

[16] D. Bivolaru, M. V. Ötügen, A. Tzes, and G. Papadopoulos, "Image Processing for Interferometric Mie and Rayleigh Scattering Velocity Measurements", AIAA Journal, Vol. 37, No. 6, pp. 688-694, 1999.

[17] D. Bivolaru, P. M. Danehy, K. D. Grinstead, Jr., S. Tedder, A. D. Cutler, "Simultaneous CARS and Interferometric Rayleigh Scattering" AIAA AMT-GT Technology Conference, San Francisco, AIAA-2006-2968 June (2006).

[18] S. Tedder, D. Bivolaru, P. M. Danehy, M.C. Weikl, F. Beyrau, T. Seeger, A. D. Cutler "Characterization of a Combined CARS and Interferometric Rayleigh Scattering System", AIAA Paper 2007-0871, 45th AIAA Aerospace Sciences Meeting and Exhibit, Reno, Nevada, January 8-11 2007.

[19] Cutler A.D., Magnotti G.,Baurle R., Bivolaru D., Tedder S., Danehy P.M., Weikl M., Beyrau F., Seeger T. " Development of Supersonic Combustion Experiments for CFD Model development" 45th AIAA Aerospace Sciences Meeting Reno, NV, Jan 2007

[20] A. D. Cutler, G. Magnotti, D. P. Capriotti and C. T. Mills, "Supersonic combusting jet experiments for code development and validation", 55th JANNAF Propulsion Meeting, Boston, MA, May 12-16, 2008

[21] P. M. Danehy, A. A. Dorrington, A. D. Cutler, R. DeLoach, "Response Surface Methods for Spatially-Resolved Optical Measurement Techniques", AIAA Ground Testing Conference, Reno NV, AIAA Paper 2003-0648, January 2003.

[22] D. Bivolaru, J. W. Lee, S. B. Jones, S. Tedder, P. M. Danehy, M. C. Weikl, G. Magnotti, and A. D. Cutler, "Mobile CARS - Rayleigh Instrument for Simultaneous Spectroscopic Measurement of Multiple Properties in Gaseous Flows", The '22nd International Congress on Instrumentation in Aerospace Simulation Facilities,' Asilomar Conference Center, Pacific Grove, California, June 10-14th 2007.

[23] S. O'Byrne, P. M. Danehy, A. D. Cutler**, "**$N_2/O_2/H_2$ Dual-pump CARS: validation experiments" 20th International Congress on Instrumentation in Aerospace Simulation Facilities, August, 2003

[24] R. P. Lucht, V. V. Natarajan, C. D. Carter, K. D. Grinstead Jr., J. R. Gord, P. M. Danehy, G. J. Fiechtner, R. L. Farrow, "Dual-pump coherent anti-Stokes Raman scattering temperature and CO2 concentration measurements," AIAA Journal Vol. 41, No. 4, April p. 679-686 2003.

[25] Bivolaru, D., Danehy, P. M., and Lee, J. W, *"Intracavity Rayleigh-Mie Scattering for multipoint, two-component velocity measurement,"* Optics Letters, Vol. 31, No. 11, pp. 1645-1647, June, 2006.

[26] M. C. Weikl, F. Beyrau, and A. Leipertz "Simultaneous temperature and exhaust-gas recirculation-measurements in a homogeneous charge-compression ignition engine by use of pure rotational coherent anti-Stokes Raman spectroscopy", Appl. Opt. Vol. 45, No. 15, 20 May 2006.

[27] K.M. Bultitude, P.M. Danehy, E. Fraval, J.S. Fox, A.F.P. Houwing "Broadband coherent anti-Stokes Raman spectroscopy (BB-CARS) in flames and hypersonic flows", 2nd Australian Conference on Laser Diagnostics in Fluid Mechanics and Combustion, Monash University, Melbourne Australia 1999.